

**CLIMATOLOGY, VARIABILITY AND EXTREMA OF OCEAN WAVES - THE  
WEB-BASED KNMI/ERA-40 WAVE ATLAS**

**Andreas Sterl**

Royal Netherlands Meteorological Institute (KNMI)  
De Bilt, Netherlands  
e-mail: sterl@knmi.nl

**Sofia Caires\***

Royal Netherlands Meteorological Institute (KNMI)  
De Bilt, Netherlands  
and Meteorological Service of Canada  
Climate Research Branch  
Downsview, Ontario, Canada

**ABSTRACT**

The European Centre for Medium Range Weather Forecasts (ECMWF) has recently finished ERA-40, a reanalysis covering the period September 1957 to August 2002. One of the products of ERA-40 consists of 6-hourly global fields of wave parameters like significant wave height and wave period. These data have been generated with the Centre's WAM wave model. From these results the authors have derived climatologies of important wave parameters, including significant wave height, mean wave period, and extreme significant wave heights. Particular emphasis is on the variability of these parameters, both in space and time. Besides for scientists studying climate change, these results are also important for engineers who have to design maritime constructions. This paper describes the ERA-40 data and gives an overview of the results derived. The results are available on a global  $1.5^\circ \times 1.5^\circ$  grid. They are accessible from the web-based KNMI/ERA-40 Wave Atlas at <http://www.knmi.nl/waveatlas>.

**INTRODUCTION**

The European Centre for Medium-Range Weather Forecasts (ECMWF) has recently performed ERA-40, a 45-year reanalysis (Sept. 1957 to Aug. 2002) of global meteorological variables (Uppala et al. 2005). The reanalysis was produced by ECMWF's Integrated Forecasting System (IFS) that uses variational data assimilation. As IFS employs a sea-state dependent sea surface

roughness, an ocean wind wave model is coupled to the atmosphere model. Therefore, the ERA-40 data contain the longest and most complete global wave dataset available. It is given on a  $1.5^\circ \times 1.5^\circ$  latitude/longitude grid covering the whole globe. The continuous 45-year length of the ERA-40 datasets makes it especially suitable to study climate variability and to estimate extreme values of certain wave parameters, e.g., the 100-year return wave height.

As part of the ERA-40 project we have extensively assessed the quality of the wave-related parameters and used them to build the web-based KNMI/ERA-40 Wave Atlas describing the global wave climate. This paper gives an overview of the verification work done and highlights the main features of the atlas.

The atlas contains some explanatory text, a basic description of the wind and wave climates in terms of means and variability, and wave statistics that are important in ocean engineering and naval architecture. The objective is two-fold. On the one hand, the atlas aims at providing a global description of the ocean climate by means of simple statistical measures. On the other hand, it aims at revealing the existence of decadal variability in the wave climate and showing the extent to which this variability affects the estimates of parameters such as the "100-year return significant wave height" which is used in the design of ships and of coastal and offshore structures. The information on decadal variability is also of great interest for climate (impact) research.

The wave-statistics part of the atlas complements, updates and improves the few existing and popular sources of global wave statistics, namely the Global Wave Statistics book of Hog-

---

\*Now at Delft Hydraulics, Delft, Netherlands

ben et al. (1986) and the Atlas of the ocean wind and wave climate of Young and Holland (1996). The information in Hogben et al. (1986) was derived from visual observations from Voluntary Observing Ships (VOS) and therefore suffers from the relative unreliability of visual observations and their poor spatial coverage outside the North Atlantic. The atlas of Young and Holland (1996) was created using only three years of altimeter data. Due to its length and the uniform spatial and temporal coverage the ERA-40 data offer the opportunity to improve upon these earlier sources. It is possible to obtain robust estimates of means and extremes, and time series analysis becomes feasible.

Regarding climate variability, the atlas reports and analyses the variability observed during the 45-year period covered by ERA-40, paying special attention to its effects on parameter estimates. For instance, 100-year return wave height estimates based on data from three different decades are significantly different in the North Pacific and the North Atlantic. This part of the atlas is also intended to complement current studies of ocean wave variability in limited areas, such as WASA (1998), Guedes Soares et al. (2002) and Wang and Swail (2001).

The atlas covers significant wave height ( $H_s$ ), 10-metre wind speed ( $U_{10}$ ) and mean wave period ( $T_m$ ). However, due to space limitations, this paper focuses on wave height.

## THE DATA SOURCES

### What is Reanalysis?

A weather forecast is essentially an initial value problem. Given the atmospheric state (the “weather”) at one time, the state at a later time can be calculated. The problem, however, with this simple view is that the atmospheric state is never known exactly. For large parts of the atmosphere observations are not available (remote areas, upper air), and available measurements necessarily contain errors. To overcome this problem the initial state for a weather forecast is obtained by a combination of the latest forecast and all new observations. The latest forecast has usually been initialized six hours earlier and gives a good *first guess* for the initialization of a new forecast. Most importantly, it provides a complete description of the atmosphere as by definition it has values of all relevant quantities at all grid points. The first guess is then combined with the newly available observations in a way not violating physical laws. The observations “push” the first guess towards “reality”. At ECMWF this *analysis* step costs about half of the total CPU-time needed to make a 10 day forecast, the other half being used for the time integration.

As a consequence, operational forecast centres naturally produce a complete description of the atmosphere’s state, usually four times a day. In principle, these data could be a valuable source of information for all kinds of investigation into the long-term variability of the atmosphere. However, weather forecast models (including the analysis procedure) are continually improved. Therefore, variability in the analyses is domi-

nated by model changes rather than by natural variability, making them unsuitable for variability studies. The aim of *reanalysis* is to overcome this problem of inhomogeneity. A state-of-the-art analysis system is used to repeat the analysis procedure for the past. As a result one obtains a complete description of the atmosphere over a long period of time which is free of inhomogeneities due to model changes. Unfortunately, inhomogeneities due to changes in data coverage remain.

### ERA-40

For the production of ERA-40 a version of the IFS has been used that was operational in June 2001. To make a 45-year’s integration possible, the horizontal resolution of the model has been decreased to  $T_L159$  ( $\approx 125$  km) instead of  $T_L511$  ( $\approx 40$  km) that is currently used in operations, and the 4DVAR data assimilation procedure has been replaced by the cheaper 3DVAR. A complete description of the IFS can be found at <http://www.ecmwf.int/research/ifsdocs/index.html>.

A distinguishing feature of ECMWF’s model is its coupling to a wave model. The coupling is needed because over sea the roughness length depends on the sea state (Janssen 1989, 1991). Specifically, the Charnock parameter (Charnock 1955) is not taken constant, but is a function of the whole wave spectrum. Thus wave information is a natural product of ERA-40. Starting in 1991, wave height data obtained from the altimeters on board of ERS-1 and ERS-2 are assimilated. The impact of the assimilation will be discussed.

The wave model used in IFS is the well-known WAM (Komen et al. 1994). It is a so-called third generation model in which the wave spectrum is computed by integration of the energy balance equation without any prior restriction of the spectral shape. From the full spectrum integral quantities like significant wave height or mean wave frequency are calculated. The model resolution is  $1.5^\circ \times 1.5^\circ$ , and the time step 15 minutes. At each fourth time step the actual 10-metre wind from the atmosphere model, which has a time step of 20 minutes, is passed to WAM. The new roughness length is then computed and passed back to the atmosphere model where it is used to calculate the air-sea fluxes of momentum, heat and moisture.

Output of results takes place at the common synoptic hours 00, 06, 12, and 18 UTC. A large subset of the complete ERA-40 data set, including  $H_s$ , mean wave period and mean wave direction, can be downloaded free of charge from [http://data.ecmwf.int/data/d/era40\\_daily/](http://data.ecmwf.int/data/d/era40_daily/). This subset is available on a  $2.5^\circ \times 2.5^\circ$  grid. The complete dataset at the full model resolution ( $1.5^\circ \times 1.5^\circ$ ) is available through ECMWF’s Data Service. This service is not free.

### Validation data

**Buoy measurements** Buoy observations are the most reliable wave observations, but they are limited in space and

time. Most buoys are located along the coast in the Northern Hemisphere, and are available only after 1978. We use buoy observations from the American National Data Buoy Center (NDBC-NOAA), which are freely available from <http://www.nodc.noaa.gov/BUOY/buoy.html>. The buoys are situated along the coasts of North America.

From the available NDBC-NOAA buoy locations 20 have been selected for the validations. Selection criteria were the distance from the coast and the water depth. Only deep water locations can be taken into account since no shallow water effects are accounted for in the wave model, and the buoys should not be too close to the coast in order for the corresponding grid points to be located at sea. The buoy  $H_s$  and surface wind measurements are available hourly from 20-minute and 10-minute long records, respectively. Although these measurements have gone through some quality control they are processed further using a procedure similar to the one used at ECMWF (Bidlot et al. 2002) and described in Caires and Sterl (2003). Wind speeds are adjusted to 10 m height using a logarithmic profile under neutral stability (e.g., Bidlot et al. 2002). In order to compare the ERA-40 results with the observations, time and space scales must be made compatible. The reanalysis results are available at synoptic times (every 6 hours) and each value is an estimate of the average condition in a grid cell, while the buoy measurements are local. Therefore, the reanalysis data are compared with 3-hour averages of buoy observations, 3 hours being the approximate time a long wave would take to cross the diagonal of a  $1.5^\circ \times 1.5^\circ$  grid cell at mid latitude. To get ERA-40 data at the buoy location the reanalysis data at the appropriate synoptic time are interpolated bilinearly to the buoy location.

**Altimeter measurements** While buoys provide high-quality continuous point measurements, satellite-borne altimeters provide near-global coverage, but every point is sampled only once in several (typically 10) days. We use along track quality checked deep water altimeter measurements of  $H_s$  and the normalized radar cross section ( $\sigma_0$ ) from GEOSAT, TOPEX, ERS-1, and ERS-2. The data are obtained from the Southampton Oceanography Centre (SOC) GAPS interface (<http://www.soc.soton.ac.uk/ALTIMETER>; Snaith 2000). The drift observed in TOPEX wave heights during 1997 to 1999 (cycles 170 to 235) is corrected according to Challenor and Cotton (1999), and the relation  $H_s^{buoy} = 1.05H_s^{topex} - 0.07$  (Caires and Sterl 2003) is used to make the TOPEX observations compatible with the buoy observations. The GEOSAT altimeter wave height data are increased by a factor of 1.065 according to Cotton and Carter (1996). No corrections are applied to the data from ERS-1 and ERS-2. The surface wind speed up to 20 m/s is obtained from  $\sigma_0$  using the algorithm of Gourrion et al. (2002), while for wind speeds above 20 m/s the relation of Young (1993) is used. More details can be found in Caires and Sterl (2003).

The satellite measurements are performed about every second with a spacing of about 5 to 7 km. "Super observations" are formed by first grouping together consecutive measurements crossing a  $1.5^\circ \times 1.5^\circ$  region. The satellite observation is then taken as the mean of these grouped data points. A quality control similar to the one applied to the buoy data is done. The reanalysis data are linearly interpolated in space and time to the mean location and the mean time of the altimeter observation.

## ASSESSMENT OF THE ERA-40 WAVE PRODUCT Validation

Before using the ERA-40 wave data to produce derived quantities they have been extensively validated against buoy and altimeter data. Figure 1 shows the timeseries of  $H_s$  as measured at buoy 46001 in the Gulf of Alaska ( $148.3^\circ\text{W}$ ,  $56.3^\circ\text{N}$ ) during 1988, together with the corresponding ERA-40 data. Three properties of the ERA-40 data can easily be recognized: (a) the two curves are nearly perfectly in phase, (b) low wave heights tend to be overestimated by ERA-40, and (c) high waves tend to be substantially underestimated.

These three features are not a peculiarity of the special location, but a general property of the ERA-40 wave data. Among the reasons for these deficiencies are resolution (P. Janssen, pers. communication) and a slight underestimation of high wind speeds (Caires and Sterl 2003). These reasons are, however, not sufficient to fully explain the severe underestimation of the wave heights in ERA-40.

Due to changes in the data assimilated, the characteristics of the data are not homogeneous in time. Four different periods have to be distinguished:

- P1** 09-1957 to 11-1991 (P1a) and 06-1993 to 12-1993 (P1b): no assimilation of altimeter wave height data,
- P2** 12-1991 to 05-1993: assimilation of faulty ERS-1 FDP (Fast Delivery Product) wave height data,
- P3** 01-1994 to 05-1996: assimilation of good but uncalibrated ERS-1 FDP wave height data, and
- P4** 06-1996 onwards: assimilation of ERS-2 FDP wave height data.

Figure 2 shows the timeseries of the globally averaged monthly mean  $H_s$  from ERA-40. This quantity has no physical interpretation but serves to give a synthesized picture of the data. The four periods identified above are clearly visible. This is especially true for period P2. The faulty data that were assimilated have a density function with two peaks. One of them is sharp and located around 2 m (Bauer and Staabs 1998) and corresponds to a systematic overestimation of wave heights around that value. Period P4 can also be easily identified: it starts with a positive trend and then levels off.

Caires and Sterl (2005b) have analyzed the error characteristics of the four periods in more detail. The following is a

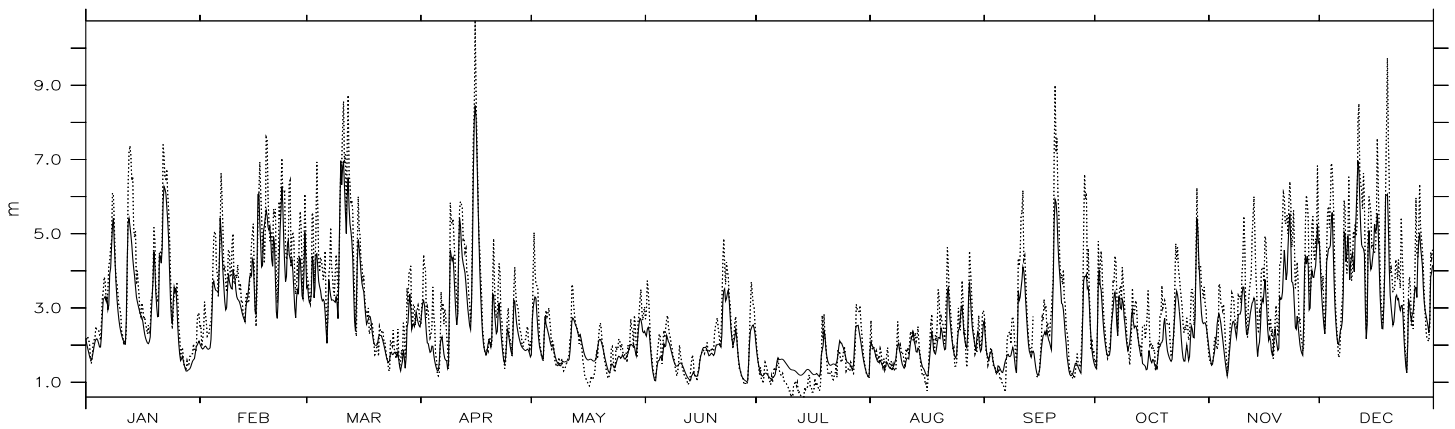


Figure 1. Measured (dotted) and modelled (solid)  $H_s$  at buoy 46001 (148.3°W, 56.3°N) in 1988.

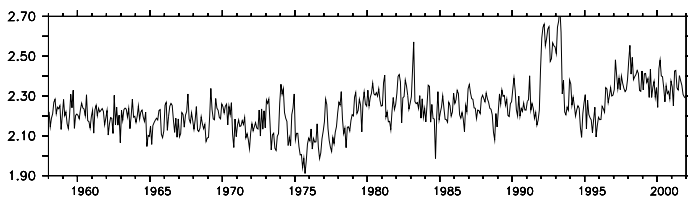


Figure 2. Timeseries of the monthly mean, globally averaged  $H_s$  from ERA-40. Monthly means are computed from the 6-hourly fields between 81°S and 81°N, and a latitudinal correction has been applied.

short summary of their findings illustrated with quantile-quantile (Q-Q) plots of buoy wave heights against ERA-40 wave heights (Figure 3). Corresponding plots using altimeter wave heights instead of the buoy measurements give essentially the same picture.

**P1** In this period the monthly mean wave fields compare well with observations, but as shown in Figure 1 ERA-40 underestimates high wave heights and overestimates the low ones. Especially the underestimation is clearly visible in the upper left panel of Figure 3.

**P2** In this period the  $H_s$  values below 3 metres are overestimated and those above are underestimated. The quality of the waves with heights above 3 m is similar to that in period P1. The Q-Q plot of ERA-40 data versus buoy data (upper right panel of Figure 3) clearly shows the overestimation for values between 1 and 3 metres that is due to the peak in the distribution function of the ERS-1 FDP mentioned above.

**P3** In this period the known calibration correction to the ERS-1 FDP data was not applied because, although it would have improved the analyzed  $H_s$  data, it would have given poorer, too high, mean wave periods. The quality of the wave height data is therefore similar to that of the data in period P1, though it has a lower scatter index (rms error normalized by the mean; not shown).

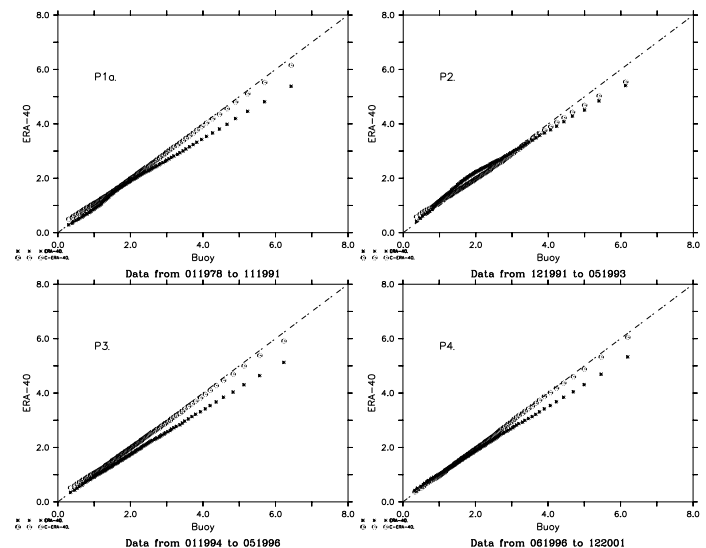


Figure 3. Quantile-quantile plots of  $H_s$  from the 20 selected buoys against collocated ERA-40 values for the different periods indicated. Asterisks: raw ERA-40 data, circles: corrected data (to be discussed later).

**P4** The assimilation of the ERS-2 FDP measurements of wave height during P4 has improved the analyzed  $H_s$ , especially in the tropics. The underestimation of high wave heights and the slight overestimation of low wave heights by the ERA-40 dataset, however, continues in this period, as is clearly seen in the lower right panel of Figure 3.

### Estimation of extreme significant wave heights

For safety considerations it is important to know extreme wave heights, i.e., wave heights that are, on average, exceeded only once per 20, 50, or 100 years. Despite the ERA-40 wave heights' inability to capture high waves the data set proved an in-

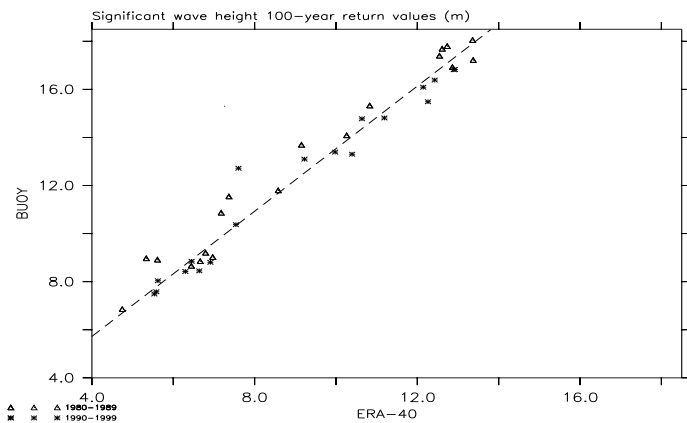


Figure 4. Linear correlation between 100-year return value estimates of  $H_s$  from buoy data and from ERA-40. The dashed line is eq. (1).

valuable basis to obtain global estimates of these extremes. Note that only extremes of significant wave height rather than those of individual waves can be obtained from the ERA-40 data.

To estimate return wave heights we used the Peak-Over-Threshold (POT) method (e.g., Coles 2001) rather than the usual fit of a distribution function. There are no good theoretical arguments as to what distribution that fit should be. In the POT method, a threshold is chosen. Whenever wave height exceeds that threshold for a period of time, the highest exceedence within that period is recorded. On theoretical grounds the exceedences must fit the two-parameter Generalized Pareto Distribution (GPD). As a special case the GPD contains the exponential distribution, which has only one parameter. Statistical tests show that the observed distribution of the exceedences cannot be distinguished from an exponential one. Therefore, an exponential distribution was fitted to the exceedences to obtain the return values. After some trial and error the 93% quantile was chosen as the threshold at each grid point.

Doing so both for buoy measurements and for the ERA-40 data results in a linear relation between the 100-year return significant wave heights ( $X_{100}$ ) obtained from both sources:

$$X_{100}^{buoy} = 0.52 + 1.30X_{100}^{ERA-40}. \quad (1)$$

This relation is illustrated in Figure 4. More details can be found in Caires and Sterl (2005a).

Buoy locations are very unevenly distributed in space, and the largest value of  $X_{100}$  found at the buoy locations is about 17 m (Figure 4). Therefore it would be preferable to have a relation between  $X_{100}$  estimates from ERA-40 and from satellites, respectively. However, satellites cross a given point only once in typically 10 days. Together with the relative shortness of the satellite

record this gives too few data for a reliable extreme-value estimate. Especially, the average number of exceedences per year cannot be determined. However, as far as parts of the estimation procedure were possible with satellite data their results are not incompatible with (1), and we therefore apply (1) globally and for all values of  $X_{100}$ .

Figure 5 shows the  $X_{100}$  values obtained by applying the POT method to the ERA-40 data and correcting the results using (1). Obviously, the highest values occur in the North Atlantic. One might suspect this to result from observation density being higher in the North Atlantic than in the Southern Ocean. While this is true for the early years, due to satellites data density is comparable in both areas towards the end of the ERA-40 period, but still the return values are highest in the North Atlantic (Figure 5, lower right panel). While mean wave heights are not higher in the North Atlantic than they are in the North Pacific or in the Southern Ocean (see Figure 6 below), the North Atlantic shows the highest variability as measured, e.g., by the inter-monthly standard deviation (not shown). In other words, conditions in the Southern Ocean are always rough, while in the North Atlantic you can be lucky and the sea is calm even in winter, or you find yourself between the highest waves possible on earth.

Some care has to be taken in interpreting the maps in Figure 5. First, ERA-40 values represent 6-hourly averages over a  $1.5^\circ \times 1.5^\circ$  area. The time and space scales of the buoy data have been made compatible with this model scale as described above. Therefore, the extreme values depicted in Figure 5 are for those scales, and much higher waves on smaller spatial and temporal scales must be expected. Secondly, the version of the WAM model used for ERA-40 does not contain shallow-water effects. Therefore, Figure 5 is not valid along the coasts. Finally, tropical storms are not properly resolved on a  $T_L 159$ -grid. In regions of tropical cyclones extreme wave heights are therefore expected to be higher than shown in the figure.

### Correction of ERA-40 data

Two main limitations of the ERA-40  $H_s$  data have been identified. The existence of inhomogeneities in time (see Figure 2) limits the use of the data for studies of climate variability and trends, and the underestimation of high wave heights (Figure 1) discourages the use of the data in design studies where the good description of the data in all ranges is important.

Inspection of time series at buoy locations such as Figure 1 led us to the conclusion that the disagreement between modeled and observed  $H_s$  is similar in similar situations. Based on this observation we proposed a new approach to improve the ERA-40 significant wave height fields. It is based on nonparametric estimation (Caires and Sterl, 2005b). The idea is to estimate at each time step the error between the ERA-40  $H_s$  value and the "true" significant wave height value and then correct the data using the estimate. The first step in error-estimation is to con-

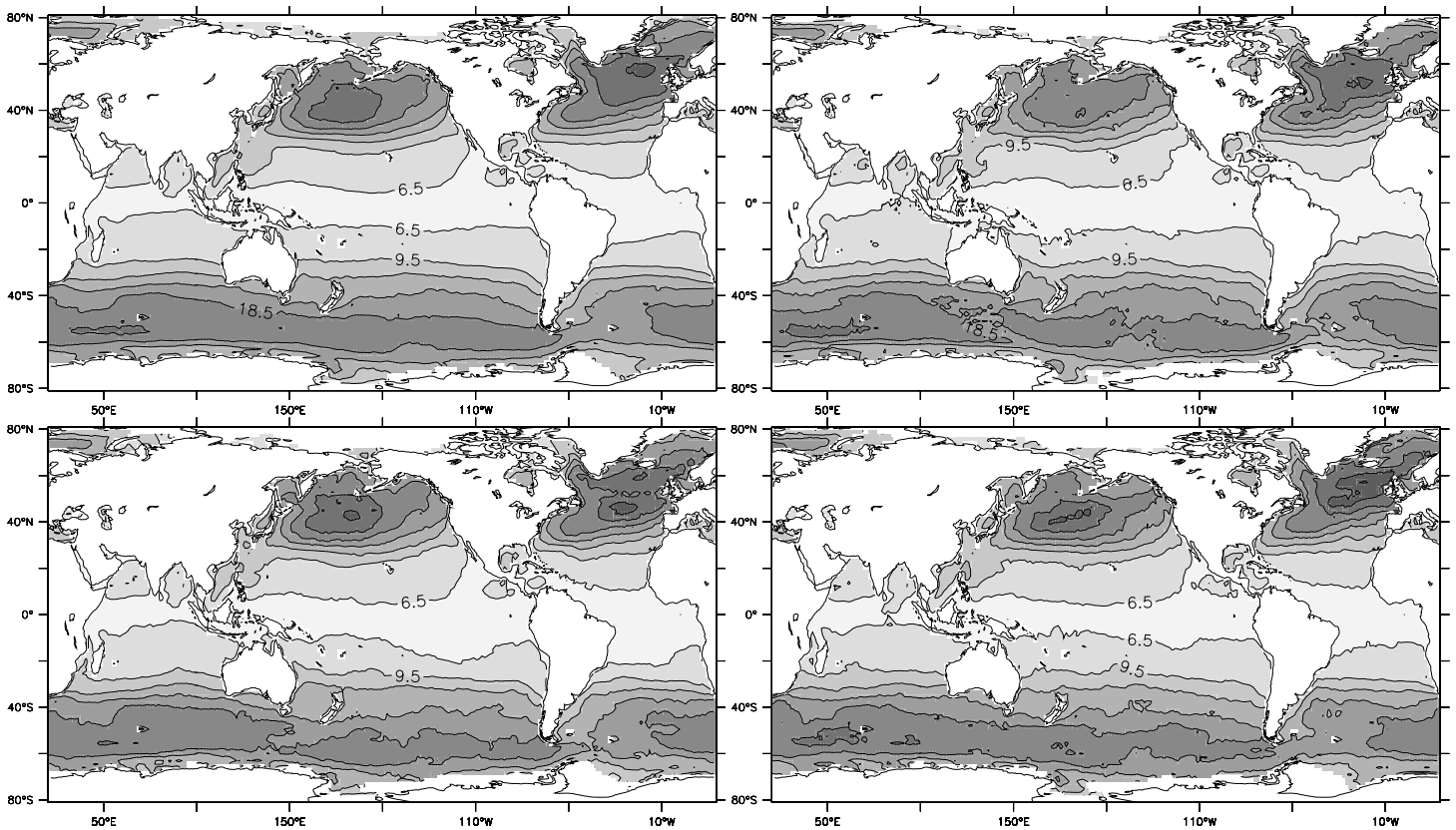


Figure 5. 100-year return  $H_s$  from ERA-40, corrected using the relationship displayed in Figure 4. Note that the results pertain to averages over  $1.5^\circ \times 1.5^\circ$ , that shallow water effects are not included, and that tropical cyclones are not resolved in ERA-40. The upper left panel is for the whole ERA-40 period (1958-2000), while the other panels are derived from three 10-year sub-periods as indicated. These panels are discussed later.

struct a “learning dataset” by collecting the discrepancies between model and “truth”, the latter being represented by collocated TOPEX measurements. This is done separately for each of the four periods P1-P4 to account for the inhomogeneities. The second step is to find for each model time step “similar” situations in the learning dataset and to use the errors to correct the model value. Usually several similar situations are found, so that also a confidence interval around the corrected data can be given. Trying several possibilities the most efficient way to define “similar” was found to require that the last 3 consecutive values of  $H_s$  are close together. For more details see Caires and Sterl (2003b).

Using this method we created a new 45-year global 6-hourly dataset—the C-ERA-40 dataset. Comparisons of the C-ERA-40 data with measurements from in-situ buoy and global altimeter data show clear improvements in both bias, scatter and quantiles in the whole range of values, as well as the removal of the inhomogeneities that are due to changes in altimeter wave height assimilation. This can be seen from the Q-Q plots in Figure 3, which contain the results from both the original ERA-40 data

and from C-ERA-40, as well as from a comparison of the global-mean  $H_s$  from ERA-40 (Figure 2) and from C-ERA-40 (Figure 8 below). The plots show that the nonparametric correction works effectively in the whole range of  $H_s$  values and for all periods.

## SOME HIGHLIGHTS FROM THE KNMI/ERA-40 WAVE ATLAS

The atlas is divided into 5 main parts: introduction and background; description of the data sources; data validation; description of climate and climate variability. Here we will describe in some detail how the information on climate and its variability are presented in the atlas and highlight some aspects.

### Climate

Climate is by definition the synthesis of weather conditions in a given area, characterized by long-term statistics (mean values, standard deviations, quantiles, etc.) of the meteorological elements in that area. The World Meteorological Organization

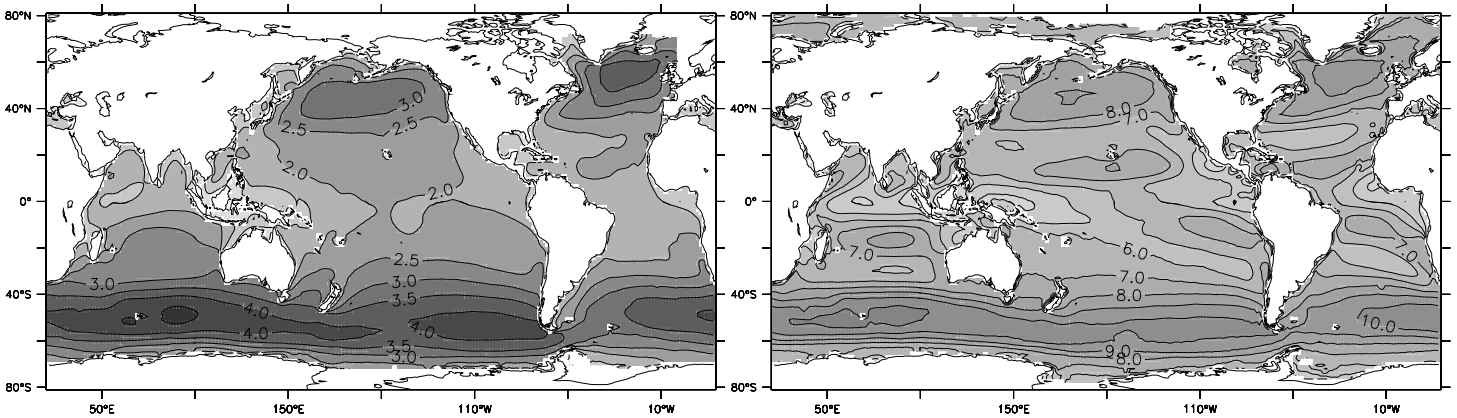


Figure 6. Annual mean climate of  $H_s$  (C-ERA-40, left, in m) and  $U_{10}$  (right, in m/s).

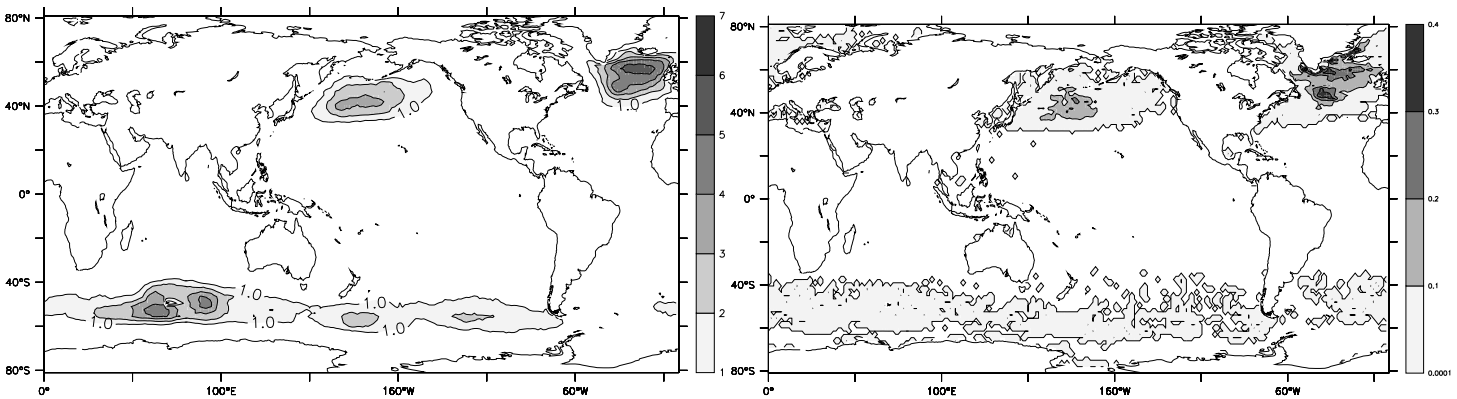


Figure 7. Mean annual exceedences of 9 m of  $H_s$  (C-ERA-40, left) and of 24 m/s of  $U_{10}$  (right) in days per year. Note that the results pertain to 6-hour averages over  $1.5^\circ$  square boxes with no wind gusts included.

(WMO) recommends climate to be based on 30 years of data. The wave climate information provided in the atlas is therefore based on the 30 years from 1971 to 2000. It includes monthly and annual means, standard deviations, 90% and 99% quantiles, the annual mean time of exceedence of certain thresholds, namely 3, 6 and 9 m for  $H_s$ , and 11, 17 and 24 m/s for  $U_{10}$ <sup>1</sup>, tabulated frequency histograms of  $H_s$  and mean wave period, and estimates of 100-year return values. The return values are based on the whole data set (not only 1971-2000) to increase their accuracy.

Figure 6 shows the annual mean climates of  $H_s$  (from the corrected C-ERA-40) and  $U_{10}$ . They are characterized by high values in the storm track regions of both hemispheres and low values in the Tropics. While the highest means occur in the Southern Hemisphere, the most extreme wave and wind conditions are found in the North Atlantic. Figure 7 shows the annual mean exceedences of the 9 m and 24 m/s thresholds of  $H_s$

and  $U_{10}$ , respectively. Exceedences are highest in the Northern Hemisphere, especially in the North Atlantic. In this region also the 100-year return value estimates of  $H_s$  (Figure 5) and  $U_{10}$  (not shown) are highest.

### Climate variability

The atlas describes the wind and wave climate variability in several ways. A short summary is provided by basin-averaged monthly-mean timeseries for seven ocean basins (global, Antarctic Ocean, Indian Ocean, South and North Pacific, South and North Atlantic). Figure 8 shows the C-ERA-40  $H_s$  and  $U_{10}$  average of monthly means over the globe using latitude correction and a smoothing of 12 months to remove the annual cycle. The most prominent feature of the  $H_s$  timeseries is a dip in September 1975 which also seems to signal a change in regime since the level of the timeseries after the dip is higher than that before. This feature is also present in the  $U_{10}$  timeseries and can be traced to the Pacific sector of the Antarctic Ocean (between  $120^\circ\text{E}$ ,  $65^\circ\text{S}$  and  $120^\circ\text{W}$ ,  $25^\circ\text{S}$ ), where  $U_{10}$  obtains its minimum.

<sup>1</sup>The thresholds for  $U_{10}$  were chosen in line with the minimum velocities of the WMO 1100 Beaufort scale for strong breeze (Beaufort 6, 10.8 m/s), gale (Beaufort 8, 17.2m/s) and storm (Beaufort 10, 24.5m/s).

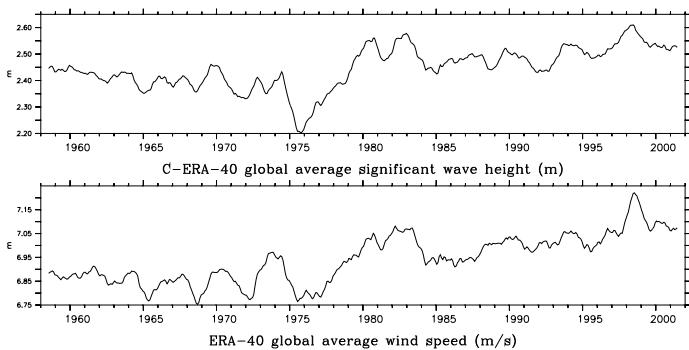


Figure 8. Timeseries of globally averaged  $H_s$  (C-ERA-40, top) and  $U_{10}$  (bottom) using latitude correction and a smoothing of 12 months to remove the annual cycle.

Due to swell propagation it affects the average of  $H_s$  over all basins with the exception of the North Atlantic (see Figure 10). We cannot trace the 1975 minimum in the timeseries to changes in the observations system of ERA-40, and therefore it is possible that it is real feature of the climate system. However, the change in the level of the timeseries before and after the minimum is most likely due to the assimilation of satellite data from 1979 onwards.

The variability is described in more detail by maps of monthly and annual anomalies of the mean and the 90% and 99% quantiles. Anomalies are calculated with respect to the period 1971 to 2000. One of the ways in which variability can be revealed is through the detection of trends. Therefore the atlas contains maps of trends of the monthly means and of the 90% and 99% quantiles. The trends vary per calendar month and from location to location, with some regions characterized by negative and other by positive trends. The trends in the 90% and 99% quantiles show the same spatial patterns as those in the mean, but have higher slopes. Maximum trends in the mean  $H_s$  are of about 4 cm/year and in the 99% quantiles of about 7 cm/year. For wind speed the upper limits are about 6 (cm/s)/year for the mean and 12 (cm/s)/year for the 99% quantiles. As an example Figure 9 shows the trends in the February monthly means and 99% quantiles from the C-ERA-40  $H_s$  data. Note that except for the North Atlantic the trends are dominated by the increase between the 1970s and the 1980s discussed above (Figure 8). The trend found in the North Atlantic and its spatial pattern are in line with the results of Günther et al. (1998).

We have used empirical orthogonal function (EOF) analysis to obtain main patterns of variability, since these patterns may be linked to possible dynamic mechanisms. The atlas presents, for each ocean basin considered, the two most important EOF patterns and their coefficient time series. Some interesting observations arise from the EOF analysis:

1. Figure 10 shows the pattern of the first global EOF of C-

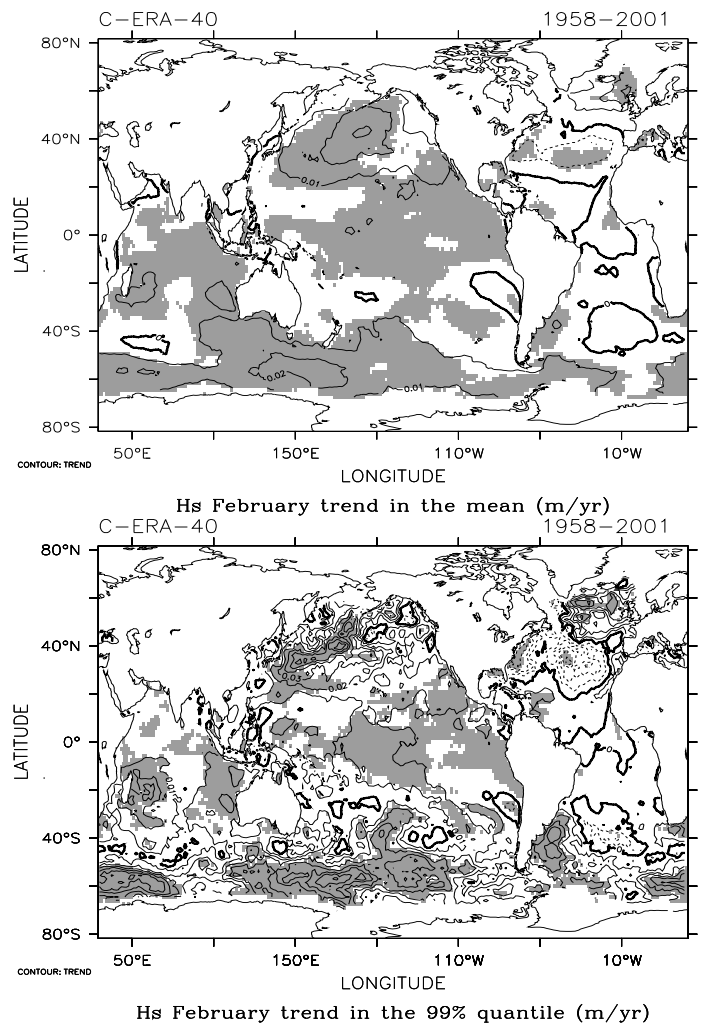


Figure 9. Trends in the February monthly mean  $H_s$  (C-ERA-40, upper) and the 99% quantiles (lower). Areas where the trend is significant at the 5% level are shaded. The significance is estimated using the non-parametric Mann-Kendall test as described in Wang, Swail (2001).

ERA-40 significant wave height. This EOF explains 15% of the global variability and clearly represents swell propagating from the Southern Hemisphere storm track region into the Indian and Pacific Oceans. Its coefficient has a correlation of about 0.8 with the global mean of C-ERA-40 significant wave height (Figure 8). In particular, it has the same dip around September 1975 as has the global curve. It illustrates the importance of the Southern Hemisphere in governing the variability of the global mean  $H_s$ .

2. The coefficient time series of the first North Pacific EOF of  $H_s$  has a correlation of about -0.76 with the Pacific-North American Index (PNA; Wallace and Gutzler 1981). It ex-



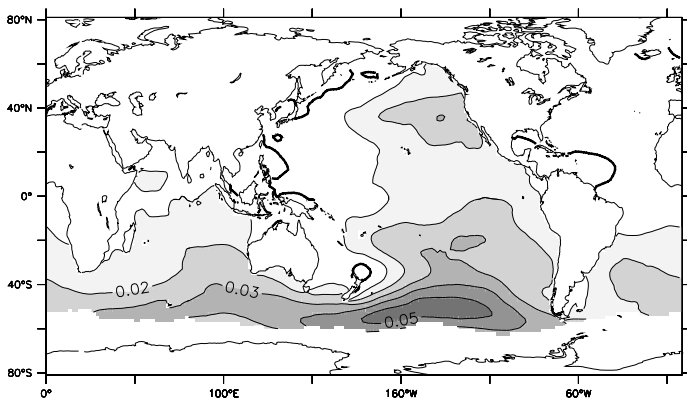


Figure 10. Pattern of the first global EOF of  $H_s$  (C-ERA-40).

plains 31% of the variability in that basin.

3. The coefficient of the second North Atlantic EOF, which explains 24% of the variability in that basin, has a correlation of about 0.8 with the North Atlantic Oscillation Index (NAO; see, e.g., Rogers 1984). The first EOF is dominated by swell and therefore not related to the NAO.

Finally, the effect of decadal climate variability on the extreme statistics, namely on the annual mean time of exceedence of certain thresholds and on the 100-year return values, is described. An example is given in Figure 5 for the corrected  $H_s$  100-year return value estimates. Besides an estimate based on the whole ERA-40 period it also contains estimates based on three different 10-year periods. The estimates obtained from these periods differ in the Northern Hemisphere storm tracks. Specifically, the estimates in the roughest part of the North Pacific storm track region have increased, and in the North Atlantic the pattern has changed. These differences can be attributed to the decadal variability in the Northern Hemisphere, especially to changes in the phase of the NAO (Caires and Sterl 2005a). This example shows that it is important to take account for climate changes when designing maritime structures.

As we have seen the  $H_s$  data reveal trends in both the monthly means and, even more pronounced, the high quantiles. There are also differences in the return values estimated with data from different decades. Changes in the monthly means and the return values can arise from *more* or from *more intense* storms. Calculating measures of storm number and storm intensity we find (Sterl and Caires 2005) that

1. There are more storms in the storm track region than in the Tropics. As we have defined storms as the roughest 10% of the time at a given place this can be interpreted as storms in the Tropics lasting longer. Note, however, that the 90% quantile is much lower in the Tropics so that a typical storm there is much less severe (remember that tropical cyclone

are not resolved!) than at higher latitudes. Therefore, it is more appropriate to conclude that the Tropics are less variable than the higher latitudes.

2. Significant changes in the number of storms occur over much larger areas than do changes in intensity.
3. In the North Atlantic only the intensity of storm changes significantly and does so only in small regions.
4. In the North Pacific both the number of storms and their intensity changes.
5. Changes in the Southern Hemisphere are mainly due to changes in the number of storms. This change, however, may be an artifact of satellite observations becoming available in 1979 (see also discussion of Figure 8).

## SUMMARY AND CONCLUSIONS

The ERA-40 reanalysis carried out at ECMWF produced 45 years (Sept. 1957 - Aug. 2002) of data describing the state of the atmosphere four times a day. ECMWF's operational model has been used to carry out the reanalysis. In this model the exchange coefficients for momentum and turbulent energy are dependent on the sea state. To achieve this, the atmosphere model is coupled to the WAM wave model. Therefore, the ERA-40 data also contain information about waves. A subset of the raw ERA-40 data can be downloaded freely from ECMWF's website at [http://www.ecmwf.int/data/d/era40\\_daily/](http://www.ecmwf.int/data/d/era40_daily/).

A thorough assessment of the ERA-40 wave height data revealed that they (a) capture very well the variability of the true wave heights on all time scales, (b) slightly overestimate low wave heights, and (c) severely underestimate high wave heights. Furthermore, inhomogeneities due to the assimilation of different data sources are clearly present.

Despite the underestimation of high wave heights it is possible to give reliable estimates of extreme significant wave heights ("100-year-return values"). Estimates based on the raw ERA-40 wave data and those from buoy measurements revealed a linear relationship that could be exploited to obtain global reliable return value estimates based on the ERA-40 data. Furthermore, it was possible to devise a non-parametric correction method to the ERA-40 data, resulting in a corrected dataset which has no bias with respect to altimeter-based wave height retrievals and which is free of obvious inhomogeneities resulting from differences in wave-height data that were assimilated.

The ERA-40 wave data have been used to create the web-based KNMI/ERA-40 Wave Atlas (<http://www.knmi.nl/waveatlas>). This atlas contains the comparisons between the ERA-40 data and observations from both buoys and satellite altimeters, the climatology of waves as deduced from both the raw and the corrected ERA-40 data, maps of exceedences as well as of return values, and an assessment of the variability of the wave climate. The latter is especially important for the derivation of the extreme statistics, as the outcome of an extreme-value analy-

sis can depend very much on the period used, with corresponding consequences for decisions based on this analysis.

## ACKNOWLEDGMENT

We are indebted to a lot of persons for their help and pleasant collaborations. Jean-Raymond Bidlot and Peter Janssen provided valuable suggestions and comments and helped with advice. Sakari Uppala and Per Kållberg as leaders of the ERA-40 production team were always open to our comments and provided valuable help in dealing with the technical aspects of the ERA-40 system. Val Swail suggested to us the production of the KNMI/ERA-40 Wave Atlas and together with Gerbrand Komen advised on its content. Helen Snaith helped with the altimeter data. The buoy data were obtained from NDBC-NOAA (<http://www.nodc.noaa.gov/BUOY/buoy.html>). The plotting was done with the free Ferret software developed by NOAA/PMEL/TMAP. Camiel Severijns provided software support. An INTAS grant (01-2206) facilitated discussions with Sergey Gulev, David Woolf and Roman Bortkovskii. This work was funded by EU as part of the ERA-40 project (no. EVK2-CT-1999-00027).

## REFERENCES

- Bauer, E., and Staabs, C., 1998. "Statistical properties of global significant wave heights and their use for validation", *J. Geophys. Res.*, Vol. 103, No. C1, pp. 1153-1166.
- Bidlot, J.-R., Holmes, D.J., Wittmann, P.A., Lalbeharry, R., and Chen, H.S., 2002. "Intercomparison of the performance of operational wave forecasting systems with buoy data", *Weather and Forecasting*, Vol. 17, pp. 287-310.
- Caires, S., and Sterl, A., 2003. "Validation of ocean wind and wave data using triple collocation", *J. Geophys. Res.*, Vol. 108, No. C3, p. 3098, doi:10.1029/2002JC001491.
- Caires, S., and Sterl, A., 2005a. "100-year return value estimates for wind speed and significant wave height from the ERA-40 data", *J. Clim.*, Vol. 18, No. 7, pp. 1031-1048.
- Caires, S., and Sterl, A., 2005b. "A new nonparametric method to correct model data: Application to significant wave height data from the ERA-40 reanalysis", *J. Oc. At. Tech.*, Vol. 22, No. 4, pp. 443-459.
- Challenor, P., and Cotton, P.D., 1999. "Trends in TOPEX significant wave height measurement", Available as PDF document at <http://www.soc.soton.ac.uk/JRD/SAT/TOPTren/TOPTren.pdf>.
- Charnock, H., 1955. "Wind stress on a water surface", *Q. J. Royal Meteorol. Soc.*, Vol. 81, pp. 639-640.
- Coles, S., 2001. "An introduction to statistical modeling of extreme values", Springer Texts in Statistics, Springer-Verlag UK.
- Cotton, P.D., and Carter, D.J.T., 1996. "Calibration and validation of ERS-2 altimeter wind/wave measurements", Southampton Oceanography Centre, Internal Document 12, 119 pp, Unpublished manuscript (D.R.A. I.T.T. CSM/078).
- Gourrion, J., Vandemark, D., Bailey, S., Chapron, B., Gommenginger, C.P., Challenor, P.G., and Srokosz, M.A., 2002. "A two parameter wind speed algorithm for Ku-band altimeters", *J. At. Oc. Tech.*, Vol. 19, No. 12, pp. 2030-2048.
- Guedes Soares, C., Weisse, R., Carretero, J.C., and E. Alvarez, 2002. "A 40 years hindcast of wind, sea level and waves in European waters", *Proceedings of the 21st International Conference on Offshore Mechanics and Arctic Engineering*, Oslo, Norway, Paper OMAE2002-28604.
- Günther, H., Rosenthal, W., Stawarz, M., Carretero, J.C., Gomez, M., Lozano, I., Serano, O., and Reistad, M., 1998. "The wave climate of the Northeast Atlantic over the period 1955-94: The WASA wave hindcast", *Global Atmos. Ocean System*, Vol. 6, pp. 121-163.
- Hogben, N., Da Cunha, N.M.C., and Oliver, G.F., 1986. "Global Wave Statistics", Unwin Brothers, London, 661 pp.
- Janssen, P.A.E.M., 1989. "Wave-induced stress and the drag of air flow over sea waves", *J. Phys. Oceanogr.*, Vol. 19, pp. 745-754.
- Janssen, P.A.E.M., 1991. "Quasi-linear theory of wind wave generation applied to wave forecasting", *J. Phys. Oceanogr.*, Vol. 21, pp. 1631-1642.
- Komen, G.J., Cavaleri, L., Donelan, M., Hasselmann, K., Hasselmann, S., and Janssen, P.A.E.M., 1994. "Dynamics and Modelling of Ocean Waves", Cambridge University Press, Cambridge, 532 pp.
- Rogers, J.C., 1984. "The association between the North Atlantic Oscillation and the Southern Oscillation in the Northern Hemisphere", *Mon. Wea. Rev.*, Vol. 112, pp. 1999-2015.
- Snaith, H.M., 2000. "Global Altimeter Processing Scheme User Manual", Southampton Oceanography Centre, 44 pp.
- Uppala, S., et multi, 2005. "The ERA-40 Re-Analysis", *Q. J. Roy. Meteor. Soc.*, Vol. 131, pp. 2961-3012.
- Wallace, J.M., and Gutzler, D.S., 1981. "Teleconnections in the geopotential height field during the Northern Hemisphere Winter", *Mon. Wea. Rev.*, Vol. 109, pp. 784-812.
- Wang, X.L., and Swail, V.R., 2001. "Changes of extreme wave heights in Northern Hemisphere oceans and related atmospheric circulation regimes", *J. Clim.*, Vol. 14, pp. 2204-2221.
- WASA Group, 1998. "Changing waves and storms in the Northeast Atlantic?", *Bull. Am. Meteorol. Soc.*, Vol. 79, pp. 741-760.
- Young, I.R., and Holland, G.J., 1996. "Atlas of the oceans: wind and wave climate", Pergamon.
- Young, I.R., 1993. "An estimate of the Geosat altimeter wind speed algorithm at high wind speeds", *J. Geophys. Res.*, Vol. 98, No. C1, pp. 20275-20285.